Vibration-compensated interferometer for surface metrology

Chunyu Zhao and James H. Burge

An advanced interferometer was built for surface metrology in environments with severe vibration. This instrument uses active control to compensate for effects of vibration to allow surface measurement with high-resolution phase-shifting interferometry. A digital signal processor and high-speed phase control from an electro-optic modulator allows phase measurements at 4000 Hz. These measurements are fed back into a real-time servo in the digital signal processor that provides a vibration-corrected phase ramp for the surface measurements taken at video rates. Unlike fringe locking, which compensates vibration to keep the phase constant, we show a true phase servo that allows the phase to be stabilized while it is ramped, enabling surface measurements using phase-shifting interferometry that requires multiple images with controlled phase shifts. © 2001 Optical Society of America

OCIS codes: 120.3180, 120.3930, 120.5050, 220.4830.

1. Introduction

The phase-shifting interferometer is frequently used for surface measurements because of its high accuracy and high spatial resolution. The fact that it has to measure sequential frames while controlling phase during a period of time makes it vulnerable to external vibration. Vibration can cause errors in surface measurement and if severe enough will completely wash out fringes. This is particularly true during testing of large mirrors where it is impossible to put the interferometer and the mirror on the same optical table.

There are a number of ways to reduce the effect of vibration on surface measurement with a phase-shifting interferometer. The most straightforward one is to reduce the time over which the data frames are collected.[1] A high-speed CCD camera and frame grabber are used in this method. Another solution to the vibration problem is to take all the required data frames simultaneously[2]; then a surface map is generated. Yamaguchi *et al*.[3] used a spatial filter and a detector to detect fringe movement, and the signal is fed back into a piezoelectric-transducer-driven reference mirror as part of a servo loop. Although good results are produced, the technique is limited to only certain fringe spacings.[3] Deck developed another solution.[4] Here the fringes are amplitude split into two detectors, one with high temporal and low spatial resolution and the other with low temporal and high spatial resolution. The high-temporal-resolution data are used for accurate calculation of the phase-step increment in the high-spatial-resolution data; then a special algorithm is used to generate the surface map. The topographic maps benefit from the best qualities of both data sets—vibration insensitivity and high spatial resolution.

This paper presents an effective and inexpensive solution to the vibration problem. We use a closed-loop servo system for actively measuring the instantaneous phase. If vibration is detected, then a command is given to the phase shifter to compensate for it. The servo maintains the phase at a specified value rather than just stabilizing the fringes. Section 2 of this paper gives a detailed description of the vibration-compensation method. Section 3 shows the layout of the interferometer we built with the vibration-compensation servo. We use an electro-optic modulator (EOM) as the phase shifter in the interferometer, and Section 4 explains how it works and why we use it. In Section 5 the high-speed phase measurement—the core of the vibration-compensation method—is justified. We analyze the performance limitations and error sources of the interferometer in Section 6. The experimental result

C. Zhao (czhao@u.arizona.edu) and J. H. Burge (jburge@as.arizona.edu) are with the Optical Sciences Center, University of Arizona, 1630 E. University Boulevard, Tucson, Arizona 85721.

Received 21 February 2001; revised manuscript received 30 July 2001.

0003-6935/01/346215-08$15.00/0

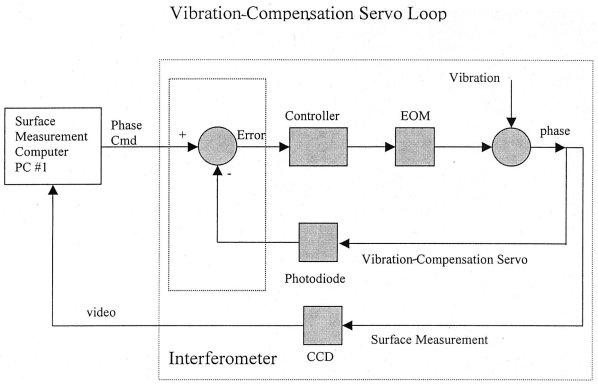

Fig. 1. Illustration of basic vibration servo. The active element, EOM, makes a correction in response to external inputs (from the surface-measurement computer and vibration) to the system.

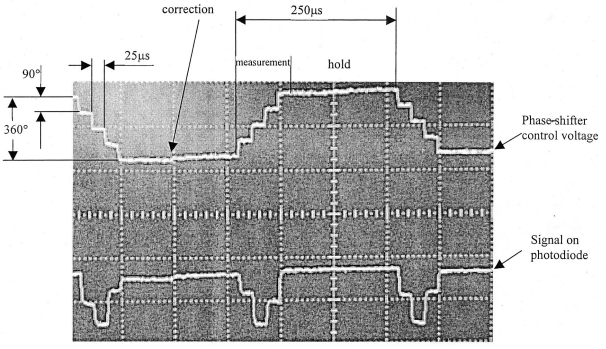

Fig. 2. Traces of the phase-shifter control signal and the signal on the photodiode for the vibration-compensation servo.

that proves that the interferometer can successfully compensate for vibration is shown in Section 7.

2. Method Description

The interferometer we describe uses two nested phase-shifting systems that use the same phase shifter, but at different frequencies. One is the high-speed system, which conducts a five-bucket measurement of phase with a single photodiode. This is used for the phase servo to measure and correct for vibration. The other is a low-frequency surface-measurement system, which initiates a ramp and measures the surface figure with use of a CCD array. The high-speed servo drives the phase to track this low-frequency ramp. Figure 1 shows the block diagram of the two systems. Both systems use the same phase shifter.

The vibration-compensation servo system consists of three main components—phase shifter, photodiode, and digital signal processor (DSP). The essential feature of the servo is the high-frequency phase measurement. The DSP sends out a phase-shifting control voltage for quick ramping of the phase by 2π, during which the intensities are measured and digitized every $\pi/2$ with the high-speed photodiode. These intensities are fed back into the DSP, and a five-step algorithm is used to calculate the phase. This cycle takes 100 μs. If deviation (due to vibration) from the phase command is detected, a correction is made to the phase-shifting control voltage to compensate for the deviation. Next the phase control voltage is held constant for 150 μs followed by a 2π shift in the opposite direction; the phase is then calculated, and vibration is compensated just like in the previous cycle (see Fig. 2). In this way the system is measuring the phase and then compensating for vibration at a frequency of 4000 Hz.

For making surface measurements with phase-shifting interferometry the servo tracks a command signal from a computer with the surface-measurement software. The surface-measurement software does not have any interaction with the vibration-compensation system other than supplying the control signal and using the stabilized images. The high-speed servo compensates for the phase noise from vibration and drives the phase to track the command. The vibration-compensation servo is running all the time; when a surface-measuring cycle starts, the phase-shifting control signals for the two systems are superimposed (see Fig. 3).

The surface-measurement system, which uses a CCD, does not see the high-frequency phase shift, because the pixel intensities are integrated for 16 ms and high-frequency measurement occurs every 0.25 ms. The high-frequency part is just averaged out and causes a reduction in fringe contrast only. Since the surface measurement never sees the servo, the interferometer can be used with any phase-measuring software. Thus we can use standard phase-shifting interferometry for surface measurements by calculating phase at each point in the array. See Fig. 3 for the phase command structure when the surface measurement is in process.

Since high-frequency phase measurements are needed to close the servo loop, both the phase shifter and the photodiode require rapid response. We use a ConOptics 380c EOM as the phase shifter. Its 3-dB cutoff frequency is 250 kHz. The photodiode is a New Focus 2001. It has a frequency response greater than 200 kHz.

3. System Description

We implement the vibration-compensation mechanism in a Twyman–Green interferometer. Figure 4 shows the layout of the interferometer. The vibration-compensation servo loop and the surface-measurement loop are clearly marked. With different choice of diverger lens, the interferometer can test different types of optics.

4. Electro-Optic Modulator

The key component of this interferometer is the EOM. Cole *et al*. used an acousto-optic modulator (AOM) as the phase shifter to build his interferometer with the same vibration-compensation device.[5,6] The AOM shifts phase by changing the frequency of the light. Compared with the AOM, the EOM has advantages of higher light efficiency, easier align-

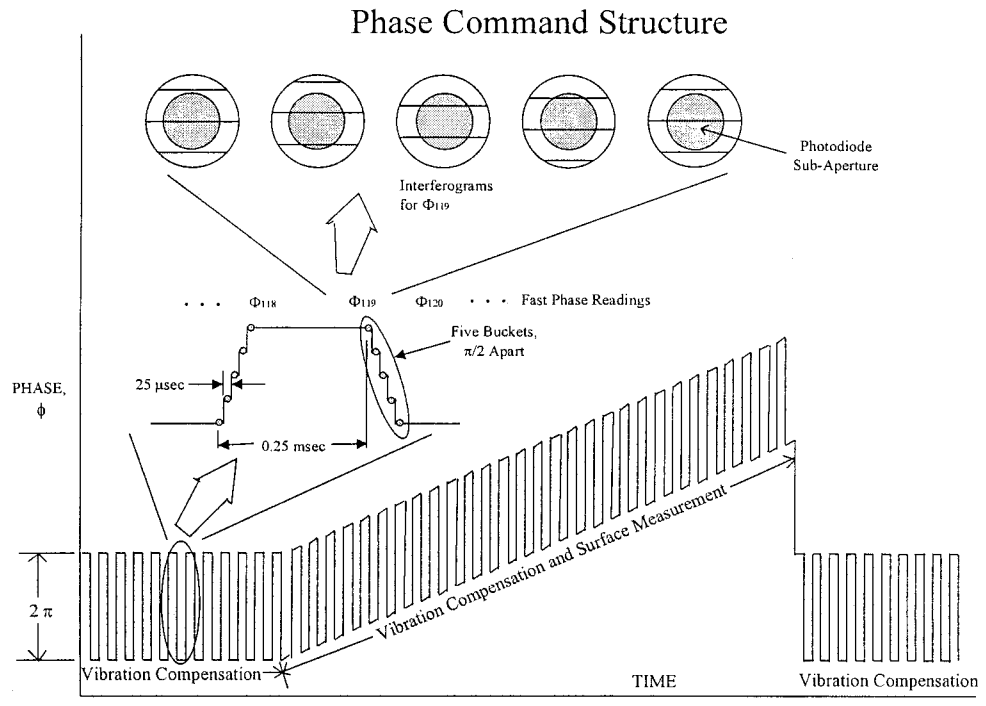

Fig. 3. Basic phase command structure for the vibration-compensation method. The photodiode intensities are used to calculate phase errors at 4000 Hz. During a surface measurement, a ramp is initiated and an integrating bucket technique is used to calculate a phase map (this picture is taken from Cole's thesis[5]).

ment, and phase shift's independence on the path-length difference between reference and test arms.

The ConOptics 380C EOM used in this interferometer is made of ammonium dihydrogen phosphate (ADP) crystal and works on transverse modulation (Fig. 5). The crystal is characterized by the following parameters: height W, length d, index of refraction for the ordinary light n_o, and index of refraction for the extraordinary light n_e. When a voltage V is applied across the ADP crystal along the z axis (the

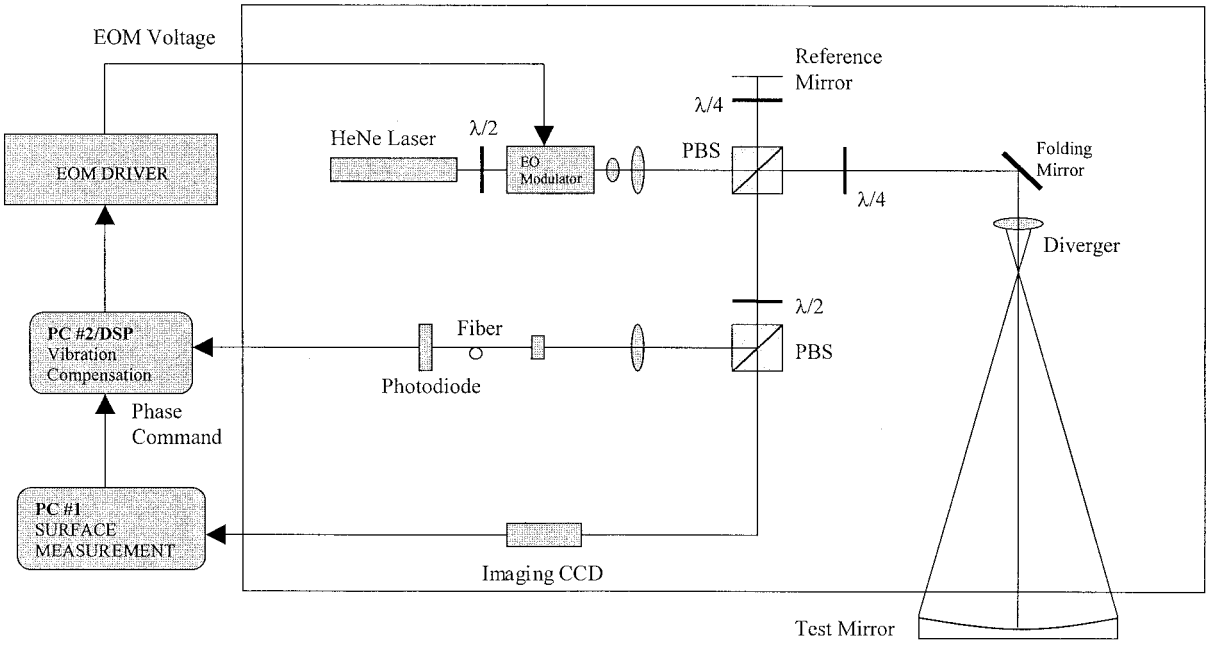

Fig. 4. Layout of the interferometer.

optical axis of the crystal), for the x-polarized light, the index of refraction is then[7]

$$n_x = n_o - \frac{1}{2} n_o^3 p_{63} \frac{V}{W}, \tag{1}$$

where p_{63} is one element of the Pockels coefficient array of the crystal. For the z-polarized light the index of refraction does not change; i.e.,

$$n_z = n_e. \tag{2}$$

Then the phase change between the x- and the z-polarized light that is due to the electrical field is

$$\begin{aligned}\Delta\phi &= \phi_z - \phi_x \\ &= \frac{2\pi}{\lambda} \frac{1}{2} n_o^3 p_{63} \frac{d}{W} V.\end{aligned} \tag{3}$$

So, for a given EOM, the phase modulation is proportional to the external voltage V. The voltage that makes $\Delta\phi = \pi$ is called the half-wave voltage, denoted as $V_{1/2}$. For the ConOptics 380c, $V_{1/2} = 116$ V for 633-nm He–Ne laser light. The EOM driver's output ranges from -400 to $+400$ V, which allows more than three waves phase shift. The dynamic range is large enough for our application.

5. High-Speed Phase Measurement

The vibration is detected by a high-speed phase measurement using a photodiode. Even though the photodiode is a single-point detector, it looks at the whole interferogram or a large subarea of it (see Figs. 3 and 4). In this section we show that we can still use phase-shifting interferometry to conduct the measurement.

Assume that the irradiance at a point (x, y) in the interferogram is $A(x, y)$, and

$$A(x, y) = A_1(x, y) + A_2(x, y)\cos[\phi(x, y) + \alpha], \tag{4}$$

where $\phi(x, y)$ is the phase difference between the two interfering beams, α is the phase-shift angle, $A_1(x, y)$ is the average irradiance, and $A_2(x, y)$ is the modulation as the phase is shifted. Then the signal the photodiode sees is I,

$$\begin{aligned}I &= \iint A(x, y)\mathrm{d}x\mathrm{d}y \\ &= \iint A_1(x, y)\mathrm{d}x\mathrm{d}y \\ &\quad + \left\{\cos\alpha \iint A_2(x, y)\cos[\phi(x, y)]\mathrm{d}x\mathrm{d}y \right. \\ &\quad \left. - \sin\alpha \iint A_2(x, y)\sin[\phi(x, y)]\mathrm{d}x\mathrm{d}y\right\} \\ &= I_1 + I_2\cos(\gamma + \alpha),\end{aligned} \tag{5}$$

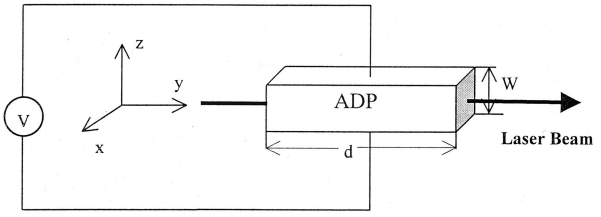

Fig. 5. EOM is the phase shifter of the interferometer.

where

$$I_1 = \iint A_1(x, y)\mathrm{d}x\mathrm{d}y, \tag{6.1}$$

$$\begin{aligned}I_2 = \left(\left\{\iint A_2(x, y)\cos[\phi(x, y)]\mathrm{d}x\mathrm{d}y\right\}^2 \right. \\ \left. + \left\{\iint A_2(x, y)\sin[\phi(x, y)]\mathrm{d}x\mathrm{d}y\right\}^2\right)^{1/2},\end{aligned} \tag{6.2}$$

$$\tan(\gamma) = \frac{\iint A_2(x, y)\sin[\phi(x, y)]\mathrm{d}x\mathrm{d}y}{\iint A_2(x, y)\cos[\phi(x, y)]\mathrm{d}x\mathrm{d}y}. \tag{6.3}$$

So the signal on the photodiode is modulated in the same way as if it represented the intensity at a single point in the interferogram. It has a phase angle γ and sees the same phase-shift angle α. Then we can use phase-shifting interferometry to determine γ. If the measurement is different from the command phase, then the difference is regarded as the vibration, and a correction is made to cancel the vibration effect.

The magnitude of I_2 depends on the number of fringes in the aperture. When $I_2 = 0$, there is no contrast and the high-frequency measurement does not work. For example, if the aperture is a unit square and there are only tilt fringes, let the fringe visibility be 1 and $\phi(x, y) = 2\pi\alpha x$ where α is the amount of tilt in waves; we can then calculate the contrast I_2/I_1 of the signal that the photodiode sees:

$$\frac{I_2}{I_1} = \left|\frac{\sin(\alpha\pi)}{\alpha\pi}\right|. \tag{7}$$

We plot the contrast as a function of α in Fig. 6. For the vibration compensation to work, the zero contrast must be avoided. This can always be done by means of increasing or decreasing the tilt in the interferogram. In practice, the vibration compensation was never limited by the contrast of the photodiode signal when we used the interferometer to test optics. A contrast of 5% or so is adequate, and we were always able to maintain it without any extra effort.

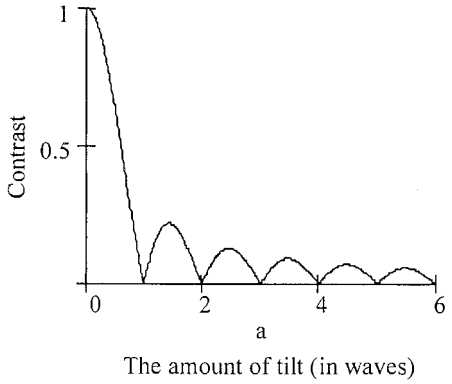

Fig. 6. Plot of the contrast of the photodiode signal for square detector versus the amount of tilt in the interferogram. We have shown system performance with no degradation with a contrast of 0.05.

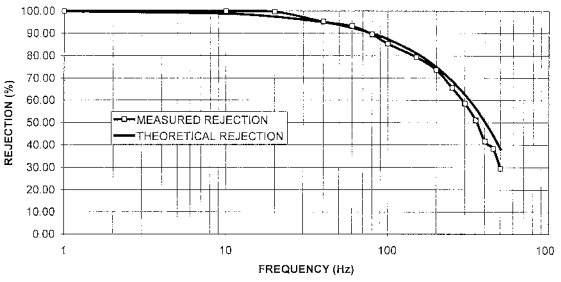

Fig. 7. Comparison of the theoretical and the measured vibration-rejection percentages for 4-kHz system operation (measured vibration rejection data is taken from Cole's thesis[5]).

6. System-Performance Analysis

Since the high-speed phase measurement measures the instantaneous phase at a frequency of 4 kHz, it is unable to determine and then compensate for higher-frequency vibration. In Subsection 6.A we give the limit of this vibration-compensation mechanism. The high-speed phase measurement is superimposed with the surface measurement; then the fringe contrast in surface measurement is reduced. Subsection 6.B gives the theoretical contrast reduction in the surface measurement. A polarizing beam splitter (PBS) is used to separate the test beam and the reference beam. The finite extinction ratio of the PBS will cause error in phase measurement. Subsection 6.C shows that the error is negligible for the PBS we use. Subsection 6.D analyzes the effect of noise in the photodiode on the surface measurement.

A. Vibration-Rejection Percentage

It takes time for the servo to complete the phase measurement and then make the compensation; so the vibration compensation is not perfect. The performance of the system is approximately calculated below.

If the phase change caused by a sinusoidal vibration is ϕ_1,

$$\phi_1 = A \sin(2\pi f t), \tag{8}$$

where A is the amplitude in waves, f is the vibration frequency, and t is time. Assuming that the high-frequency phase measurement accurately determines the phase change caused by vibration, then because of the time delay in the compensation, the compensation ϕ_2 is

$$\phi_2 = A \sin[2\pi f(t - \Delta t)], \tag{9}$$

where Δt is the time delay and $\Delta t \cong 200$ μs in our case. Then the residual phase change due to vibration is

$$\Delta\phi = \phi_1 - \phi_2 = 2A \sin(\pi f \Delta t)\cos\left[2\pi f\left(t - \frac{\Delta t}{2}\right)\right], \tag{10}$$

whose amplitude is $2A \sin(\pi f \Delta t)$. So the percentage vibration rejection is

$$\text{Rejection} = 100[1 - 2 \sin(\pi f \Delta t)]. \tag{11}$$

Figure 7 shows the measured and the theoretical vibration-rejection percentage (measured vibration-rejection data is taken from Cole's thesis[5]). When the vibration frequency is low, the theoretical vibration-rejection percentage agrees with the measured one. When the vibration frequency is high, since the measured phase change due to vibration is not accurate, Eq. (11) no longer holds, and this explains the discrepancy between the measured and the theoretical vibration-rejection percentage at the high-frequency end.

Ultimately, the finite sampling frequency limits the performance of the servo. The servo measures the vibration and then compensates it at a frequency of 4 kHz; then the vibration of frequency close to or higher than 4 kHz is beyond the compensation capability of this interferometer. Even for vibration frequency less than 4 kHz, the interferometer has limitations. An error in the phase shift, which is proportional to the first derivative of the vibration, causes errors in the high-speed measurement, which directly affect the servo. For sinusoidal vibration described by Eq. (8) the first derivative is proportional to the vibration's amplitude-frequency product, Af. This interferometer can reject more than 75% of the vibration with amplitude-frequency product less than 200 wave · Hz and frequency less than 200 Hz.

B. Fringe-Contrast Reduction in Surface Measurement

Because of the averaging effect of the high-frequency phase measurement, the fringe contrast on the surface-measurement camera is reduced. With the

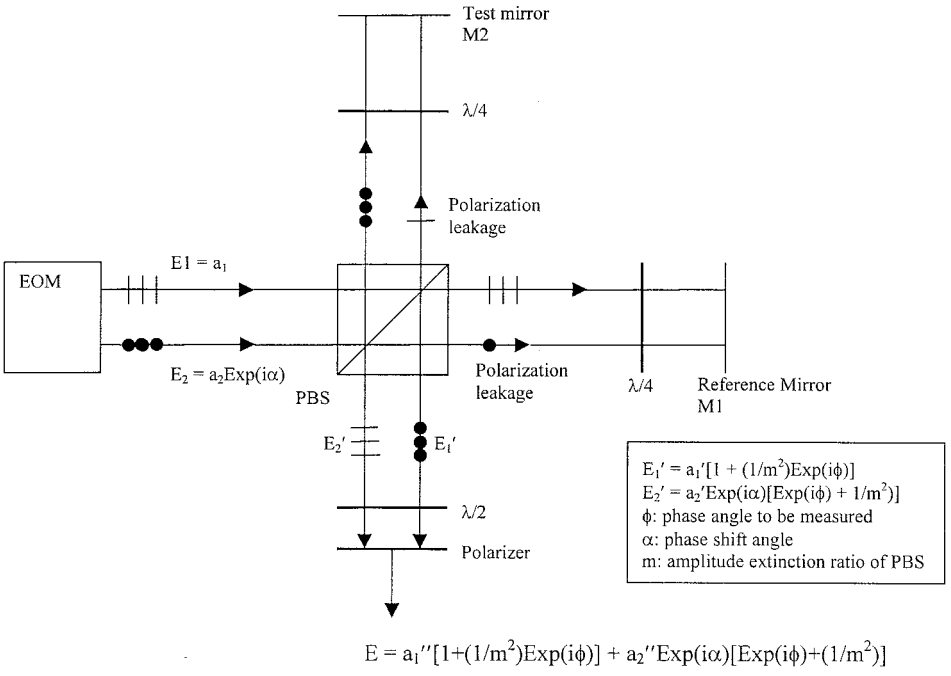

Fig. 8. Illustration of how PBS separates and then recombines the two polarizing beams. Polarization leakage is shown. α, phase-shift angle; ϕ, phase difference between the test and reference beams; m^2, intensity extinction ratio of the PBS. Dots and short bars indicate the polarizations.

vibration servo off, the contrast of the signal on the CCD is γ; then the signal on a specific pixel is

$$I = I_1(1 + \gamma \cos \phi). \tag{12}$$

When the vibration servo is on, during the high-speed phase-ramping period, the signal is just averaged out. If the duty cycle of the high-speed phase measurement is α (the ratio between the phase-ramping time and the sampling period), then the signal on the same pixel of the CCD is now

$$\begin{aligned} I' &= \alpha I_1 + (1 - \alpha) I_1(1 + \gamma \cos \phi) \\ &= I_1[1 + (1 - \alpha)\gamma \cos \phi)]. \end{aligned} \tag{13}$$

So the signal contrast is now

$$\gamma' = (1 - \alpha)\gamma, \tag{14}$$

which is reduced from the original contrast by a factor of $(1 - \alpha)$. In our case, phase ramping takes 100 μs and the sampling period is 250 μs (4 kHz); so $\alpha = 0.4$, and the fringe contrast drops 40% when the vibration servo is on compared with when it is off. This has been shown in the lab.[5]

C. Effect of Polarization Leakage of the Polarizing Beam Splitter

Several polarization components are used in this interferometer (see Fig. 4). First, the EOM shifts the phase of one polarization relative to the other; then the PBS separates the two polarizations. The PBS sends one polarization to the test arm and the other to the reference arm. Because the extinction ratio of the PBS is finite, polarization leakage occurs, which causes errors in surface measurement. Figure 8 illustrates the separation and leakage of the polarizations at the PBS. The signal the camera sees is the light irradiance I:

$$I = |E|^2 = \left| \alpha_1'' \left[1 + \frac{1}{m^2} \exp(i\phi) \right] + \alpha_2'' \times \exp(i\alpha) \left[\exp(i\phi) + \frac{1}{m^2} \right] \right|^2, \tag{15}$$

where α_1'' and α_2'' are the amplitudes of the electric fields contributed by the two polarizations, m is the amplitude extinction ratio of the PBS, ϕ is phase angle to be determined, and α is the phase-shift angle. For typical PBS, m^2 ranges from 100 to 10^5. Since $m^2 \gg 1$, we can simplify Eq. (15):

$$\begin{aligned} I &\cong \left| \alpha_1'' \exp\left(i \frac{\sin \phi}{m^2} \right) + \alpha_2'' \times \exp\left[i\left(\alpha + \phi - \frac{\sin \phi}{m^2} \right) \right] \right|^2 \\ &= |\alpha_1''|^2 + |\alpha_2''|^2 + 2\alpha_1''\alpha_2'' \cos\left(\alpha + \phi - 2 \frac{\sin \phi}{m^2} \right). \end{aligned} \tag{16}$$

Apparently the finite value of m^2 results in an error $\Delta\phi$ when ϕ is measured. Equation (16) shows that, as a function of ϕ,

$$\Delta\phi(\phi) = -\frac{2 \sin \phi}{m^2} \text{ (rad)}. \tag{17}$$

Table 1. Typical Values of the Parameters in Calculating the Residual Phase-Step Error of Surface Measurement

Parameter	Value
Laser	
Wavelength	632.8 nm
Output power	2 mW
Photodiode	
NEP	1 pW/$\sqrt{\text{Hz}}$
B	200 kHz
Servo period (Δt)	0.25 ms
CCD integration time (ΔT)	16 ms
Power on photodiode (I)	>5 μW
Contrast on photodiode (C)	>0.05
ϵ_r	
In radians	$<1 \times 10^{-4}$
In waves	$<1.6 \times 10^{-5}$

For the PBS we use, $m^2 > 1000$, the peak measurement error is less than 0.001 wave. So the polarization leakage has little effect on the measurement accuracy.

D. Error in Vibration Compensation Due to Noise in the Photodiode Signal

In Section 5 we showed that the contrast of the photodiode signal is a function of the number of fringes in the interferogram and that it might be small sometimes. The low contrast coupled with noise will result in error in the calculation of the instantaneous phase, and the effectiveness of vibration compensation will diminish. Assume that the contrast of the photodiode signal is C, the average signal is I, and the noise is N; then the signal-to-noise ratio (SNR) of the high-frequency measurement is[8]

$$\text{SNR} = \frac{CI}{N} = \frac{CI}{\text{NEP}\sqrt{B}}, \tag{18}$$

where NEP is noise-equivalent power for the photodiode and B is the noise-equivalent bandwidth. In our case, NEP = 1 pW/$\sqrt{\text{Hz}}$ and B = 200 kHz. For the five-step Hariharan algorithm that is used for high-frequency phase measurement, this SNR will cause a phase-calculation error whose standard deviation is[9]

$$\sigma_p = \frac{1}{\sqrt{5}} \frac{1}{\text{SNR}}. \tag{19}$$

In an extreme case in which contrast C = 0.05 and power I = 5 μW, σ_p is 0.0008 rad. This phase calculation is done every Δt = 0.25 ms. If the CCD camera's integration time for one frame is ΔT, which includes many cycles of phase calculation and vibration compensation, then the random phase-calculation error at each cycle will be averaged out. Assuming that the noise is uncorrelated from one measurement to the next, the residual error in the average will fall with the square root of the number of measurements averaged together. The residual noise in phase for the average is then

$$\epsilon_r = \left(\frac{\Delta t}{\Delta T}\right)^{1/2} \sigma_p, \tag{20}$$

which is the phase-step error for surface measurement. When the integration time of the CCD is T = 16 ms, the error in phase step seen by the CCD is $\epsilon_r = 1 \times 10^{-4}$ rad. If a five-bucket algorithm is used for the surface measurement, the error will be 1×10^{-8} rad, which is completely negligible.[9] Table 1 gives the numbers used for the above calculations.

7. Result

The final system specifications of the interferometer are listed in Table 2. To demonstrate the performance of the servo system, we tested a flat mirror in a room with severe vibration. The air handlers were loud, and the interferometer and the flat mirror were mounted on a nonfloating table. We used Durango software developed by Diffraction International Incorporated for the surface measurements. It was impossible to get meaningful data with the vibration servo turned off. A typical measurement without the servo, shown in Fig. 9(a), has errors of the order of 0.5 waves rms. With the vibration servo turned on, we obtain high-quality, repeatable measurements in this same environment. The map shown in Fig. 9(b) was taken in the same environment as that in

Table 2. System Specifications

Parameter	Value	Remarks
System Specifications		
Source wavelength (nm)	633	He–Ne laser
Phase sampling frequency (Hz)	4000	Limited by DSP
Operational limitations	140 Hz	80% Rejection for vibrations at this frequency
	300 wave · Hz	For vibration frequency <200 Hz
Duty cycle (%)	40	Time spent ramping 2π
Contrast on CCD (%)	60	Maximum
EO Modulator		
Half-wave voltage (V)	116	
Maximum phase shift allowed (wave)	3.4	

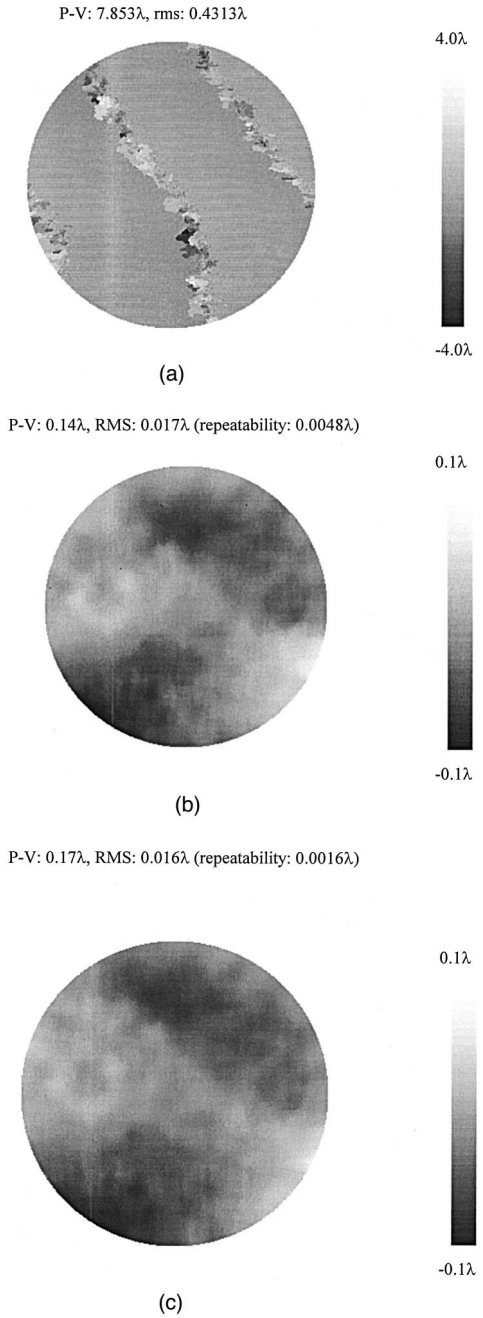

Fig. 9. Surface map made with phase-shifting interferometry for three cases: (a) in the presence of severe vibration with the servo turned off, (b) in the same severe environment with the servo operational, and (c) the same surface, measured with standard phase-shifting interferometry in a quiet environment.

Fig. 9(a), but with the vibration-compensation system. This measurement compares well with a measurement of the same optic, made under quiet conditions, shown in Fig. 9(c). The difference of the two results is less than $\lambda/1000$ for rms deviation.

8. Summary

We built a phase-shifting Twymann–Green interferometer that is capable of compensating for vibration. The basic idea is to perform high-frequency phase measurement on top of the surface measurement to detect the vibration. If vibration is detected, the phase-shift angle is either increased or decreased to cancel the vibration effect. This vibration-compensation mechanism was demonstrated to work as predicted. In an environment with severe vibration, we successfully made surface measurements with the vibration-compensation servo on. When the servo is turned off, we were not able to make measurements in the same situation.

References

1. D. L. Modisett, "Phase-shifting interferometry at high frame rates," Ph.D. dissertation (Optical Sciences Center, University of Arizona, Tucson, Ariz., 1998).
2. C. L. Koliopoulos, "Simultaneous phase shift interferometer," in *Advanced Optical Manufacturing and Testing II*, V. J. Doherty, ed., Proc. SPIE **1531,** 119–127 (1991).
3. I. Yamaguchi, J. Liu, and J. Kato, "Active phase-shifting interferometers for shape and deformation measurements," Opt. Eng. **10,** 2930–2937 (1996).
4. L. Deck, "Vibration-resistant phase-shifting interferometry," Appl. Opt. **35,** 6655–6662 (1996).
5. G. C. Cole, "Vibration compensation for a phase shifting interferometer," M.S. thesis (Optical Sciences Center, University of Arizona, Tucson, Ariz., 1997).
6. G. C. Cole, J. H. Burge, and L. Dettmann, "Vibration stabilization of a phase shifting interferometer for large optics," in *Optical Manufacturing and Testing II*, H. Stahl, ed., Proc. SPIE **3134,** 438–446 (1997).
7. M. A. Karim, *Electro-Optical Devices and Systems*, PWS-Kent Series in Electrical Engineering (PWS-Kent, Boston, Mass., 1990), Chap. 7.
8. J. M. Palmer, Optical Sciences Center, University of Arizona, Tucson, Ariz. 85721 (personal communication, 1998).
9. J. E. Greivenkamp and J. H. Bruning, "Phase shifting interferometry," in *Optical Shop Testing*, D. Malacara, ed. (Wiley, New York, 1992), pp. 501–598.